Published OnlineFirst December 8, 2009; DOI: 10.1158/1535-7163.MCT-09-0237

Angiotensin type 2 receptor–mediated apoptosis of human prostate cancer cells

Hongwei Li,[3] Yanfei Qi,[2] Chengyao Li,[3] Leah N. Braseth,[1] Yongxin Gao,[1] Arseniy E. Shabashvili,[1] Michael J. Katovich,[2] and Colin Sumners[1]

[1]Department of Physiology and Functional Genomics and McKnight Brain Institute and [2]Department of Pharmacodynamics, University of Florida, Gainesville, Florida and [3]School of Biotechnology, Southern Medical University, Guangzhou, China

Abstract

Angiotensin II (Ang II) type 1 receptor blocking drugs have been shown to inhibit the growth of prostate cancer cells and delay the development of prostate cancer. Functional Ang II type 2 receptors (AT2R) are present in these cells and inhibit growth induced by epidermal growth factor. The present studies report apoptosis of prostate cancer cells induced by AT2R overexpression. A recombinant adenoviral vector expressing AT2R (Ad-G-AT2R-EGFP) was transduced into prostate cancer cells, including androgen-independent (DU145 and PC3) and androgen-dependent cell lines (LNCaP). Following AT2R transduction, apoptosis was analyzed by terminal deoxynucleotidyl transferase–mediated dUTP nick end labeling staining and caspase-3 activity assays. The results indicate that increased expression of AT2R alone induced apoptosis in the prostate cancer lines, an effect that did not require Ang II. AT2R overexpression in DU145 cells induced inhibition of proliferation, a significant reduction of S-phase cells, and an enrichment of G_1-phase cells. The data also indicate that overexpression of AT2R led to apoptosis via an extrinsic cell death signaling pathway that is dependent on activation of p38 mitogen-activated protein kinase, caspase-8, and caspase-3. Finally, the apoptosis induced by AT2R overexpression is partially dependent on the activation of p53, but not on p21. The observations presented here suggest that the ability of increased AT2R expression to induce apoptosis in prostate cancer cells may have potential therapeutic implications for this disease, and suggest that *AT2R* is a promising novel target gene for prostate cancer gene therapy. [Mol Cancer Ther 2009;8(12):3255–65]

Introduction

Prostate cancer is the most common cancer and the second leading cause of cancer-related deaths in men in the United States (1, 2). Chemotherapy has been of limited value because most patients do not respond to secondary manipulations after developing hormone-refractory disease (3). Significant advances have been made in gene therapy, and several clinical trials have been in progress over recent years as a result of developments in molecular and cell biology (4–10). Thus, it is important to develop novel therapeutic approaches and to explore the use of gene therapy as an alternative treatment modality.

There is increasing evidence that angiotensin II (Ang II), a major physiologic regulator of blood pressure and cardiovascular homeostasis, has important pathophysiologic roles as a stimulator of cardiac hypertrophy, vascular cell proliferation, inflammation, and tissue remodeling (11). These actions, mediated via the Ang II type 1 receptor (AT1R), led to the idea that Ang II may play a role in cancer, and experimental evidence indicates that angiotensin-converting enzyme inhibitors and AT1R blockers have beneficial effects on tumor progression, vascularization, and metastasis (12–14). Further, numerous studies have shown antigrowth and antiproliferative effects of Ang II via Ang II type 2 receptor (AT2R), in opposition to actions of this peptide via the AT1R (15–18). Thus, there may be a potential beneficial role of AT2R in cancer, and this idea is supported by data that indicate that pheochromocytoma growth is inhibited by AT2R activation (19). With regard to the prostate, there is clear evidence of a tissue-based renin-angiotensin system within this gland and studies to date indicate beneficial actions of blocking AT1R and activating AT2R (15, 20–23). For example, AT1R inhibitors decrease the growth of some prostate cancer cell lines and delay the development of prostate cancer, whereas AT2R inhibitors are present and have the ability to inhibit epidermal growth factor–induced prostate cancer cell growth in LNCaP and fast-growing androgen-independent PC3 cell lines (24). Increased expression of AT2R induces apoptosis in numerous cell lines, such as pheochromocytoma, fibroblasts, smooth muscle cells, and endothelial cells, with either Ang II–dependent or Ang II–independent regulation (25–32). Thus, in the present study, we have determined

Received 3/13/09; revised 9/21/09; accepted 10/21/09; published OnlineFirst 12/8/09.

The costs of publication of this article were defrayed in part by the payment of page charges. This article must therefore be hereby marked *advertisement* in accordance with 18 U.S.C. Section 1734 solely to indicate this fact.

Note: Supplementary material for this article is available at Molecular Cancer Therapeutics Online (http://mct.aacrjournals.org/).

Requests for reprints: Colin Sumners, Department of Physiology and Functional Genomics, College of Medicine, Box 100274, 1600 Southwest Archer Road, University of Florida, Gainesville, FL 32610-0274. Phone: 352-392-4485; Fax: 352-294-0191. E-mail: csumners@ufl.edu or Hongwei Li, Department of Physiology and Functional Genomics, College of Medicine, Box 100274, 1600 Southwest Archer Road, University of Florida, Gainesville, FL 32610-0274. Phone: 352-392-9236; Fax: 352-294-0191. E-mail: hongwei1@yahoo.com

doi:10.1158/1535-7163.MCT-09-0237

Published OnlineFirst December 8, 2009; DOI: 10.1158/1535-7163.MCT-09-0237

the effects of adenoviral-induced increases in expression of AT2R on proliferation and apoptosis of prostate cancer cell lines and have addressed the potential intracellular mechanisms.

Materials and Methods

Cell Culture

Three human prostate cancer cell lines (DU145, LNCaP, and PC3) and a normal prostate stromal cell line (WPMY-1) were used in these experiments. All cell lines were obtained from the American Type Culture Collection and cultured using the protocol provided by the company. Sera and media were purchased from Invitrogen and American Type Culture Collection.

Recombinant Adenoviral Constructs

For these experiments, we constructed and prepared two recombinant adenoviral vectors as detailed previously (33): an adenoviral vector containing the enhanced green fluorescent protein gene controlled by a cytomegalovirus promoter (Ad-CMV-EGFP) and an adenoviral vector containing genomic AT2R (G-AT2R) DNA with introns 1 and 2 and the encoding region and enhanced green fluorescent protein gene controlled by cytomegalovirus promoters (Ad-G-AT2R-EGFP).

Cell Treatments

For viral transduction, prostate cancer cells (4×10^5) were seeded into six-well Nunc tissue culture plates. On the following day, cells were transduced with Ad-G-AT2R-EGFP or the control vector Ad-CMV-EGFP and changes in cell morphology were observed using an Olympus BX41 fluorescence microscope. Transduced cells were used 24 to 48 h later, depending on the specific protocol.

The role of Ang II in apoptosis elicited by increased expression of AT2R was determined as follows. DU145 cells were treated with either Ang II, an AT2R agonist, or Ang II receptor antagonists at 6 h after viral transduction, at which time Ad-G-AT2R-EGFP and Ad-CMV-EGFP have transduced into the cells but there has not been significant expression of AT2R or GFP. All treatments were repeated every 12 h to compensate for potential degradation. The number of apoptotic cells was assessed as described below.

For the p38 mitogen-activated protein kinase (MAPK) and caspase inhibitor studies, DU145 cells were transduced with Ad-G-AT2R-EGFP [100 infectious units (ifu)/cell] for 6 h followed by treatment with either the p38 MAPK-specific inhibitor SB203580, the caspase-3 inhibitor Ac-DEVD-CMK, the caspase-8 inhibitor Z-IETD-FMK, the caspase-9 inhibitor Z-LEHD-FMK, or control solvent (DMSO). All inhibitors were purchased from Calbiochem. Twenty-four hours later, the number of apoptotic cells was assessed as described below.

For the small interfering RNA (siRNA) studies, DU145 cells were transfected with either p38, p53, p21, or control siRNA using siLentFect Lipid Reagent (Bio-Rad, Inc.) following the manufacturer's protocol. All siRNAs were purchased from Qiagen. These treatments were followed 24 h later by transduction with Ad-G-AT2R-EGFP (100 ifu/cell) and then, 48 h later, assessment of the number of apoptotic cells or apoptosis-related genes/proteins as described below.

AT2R Immunostaining

Cells transduced with Ad-G-AT2R-EGFP or Ad-CMV-EGFP for 48 h were washed briefly with Dulbecco's PBS and then fixed for 10 min at 4°C with cold methanol. Immunostaining was then done on the fixed cells as detailed previously (34) using a goat anti-AT2R receptor polyclonal antibody (1:200; Santa Cruz Biotechnology) followed by Alexa Fluor 594 goat anti-rabbit IgG (1:1,000; Invitrogen) as the secondary antibody. AT2R immunoreactivity (red) and green fluorescence (from GFP) were detected using an Olympus BX41 fluorescence microscope.

Cell Proliferation and Cytotoxicity Assays

Cell proliferation and cytotoxicity were evaluated using a CytoScan WST-1 Cell Proliferation Assay (G-Biosciences). WST-1 reagent was added to the culture medium (1:10 dilution), and absorbance was measured at 450 nm.

Cell Cycle Analyses

For cell cycle analysis, samples (1×10^6 cells) were fixed and permeabilized by addition of 1 mL of ice-cold 70% ethanol for 15 min on ice. After washing, the cells were resuspended in 125 μL of 1.12% (w/v) sodium citrate containing 0.2 mg/mL RNase (Roche) and incubated at 37°C for 15 min. Next, 125 μL of 1.12% (w/v) sodium citrate containing 50 μg/mL propidium iodide (Sigma-Aldrich) were added to the cells. Following treatment for 30 min at room temperature in the dark, the cells were stored at 4°C until analysis by flow cytometry (FACSCalibur, BD Biosciences). Cell cycle analysis was done using ModFit LT software (Verity).

Apoptosis Assessment

The number of green fluorescing cells that exhibit apoptotic-like morphology was assessed by counting cells from 10 random fields per well. Counts were done by an individual who was blinded as to the treatment.

Apoptosis of viral vector–transduced cells was also measured using a DeadEnd Colorimetric terminal deoxynucleotidyl transferase–mediated dUTP nick end labeling (TUNEL) System (Promega). At 48 h after transduction, the growth medium was aspirated, and cells were fixed with 4% formaldehyde in PBS (pH 7.4) for 25 min at room temperature, then washed twice for 5 min in PBS, permeabilized in 0.2% Triton X-100 solution in PBS for 5 min at room temperature, and finally washed twice for 5 min in PBS. DeadEnd Colorimetric TUNEL System was used according to the manufacturer's instructions. Cells were mounted in Vectashield + 4′,6-diamidino-2-phenylindole (Vector Labs) to stain nuclei. The number of TUNEL-positive cells (brown color) in each treatment condition was counted from 10 random fields per well by an individual who was blinded as to the treatment. Data are presented as a percent of the total number of cells on the dish, which was assessed from 4′,6-diamidino-2-phenylindole staining.

Caspase-3–Like Protease Activity

Caspase-3–like protease activity was assessed using the BD ApoAlert caspase-3 colorimetric assay kit (BD Biosciences) as described by the manufacturer. Transduced

Published OnlineFirst December 8, 2009; DOI: 10.1158/1535-7163.MCT-09-0237

and control cells (10^6) were lysed in the lysis buffer contained in the kit followed by centrifugation (15,000 × *g* for 10 min at 4°C). Caspase-3–like activity was assessed in supernatants by following the proteolytic cleavage of the colorimetric substrate Ac-DEVD-pNA. Samples were read at 405 nm in a spectrophotometer using a 100 μL quartz cuvette. DEVD-z-DEVD-fmk, a specific inhibitor of caspase-3, was used to confirm assay specificity.

RNA Isolation and Reverse Transcription-PCR

LNCaP, DU145, and PC3 cells were cultured in their respective media and harvested for reverse transcription-PCR (RT-PCR). Total RNA was isolated from the cells using an RNeasy kit (Qiagen). Isolated RNA underwent DNase I treatment to remove genomic DNA and was then converted into cDNA with iScript cDNA synthesis kit (Bio-Rad). PCR of AT2R and glyceraldehyde-3-phosphate dehydrogenase (GAPDH) was done under the following conditions: denaturing for 30 s at 95°C, annealing for 30 s at 55°C, and extension for 30 s at 72°C, with a total of 40 cycles for AT2R and 30 cycles for GAPDH. The oligonucleotide sequences of forward and reverse primers used for AT2R were as follows: forward, 5′-CCACCCTTGCCACTACTAGCA-3′; reverse 5′-CATTGTTGCCAGAGATGTTCACA-3′. Oligonucleotide primers for GAPDH, which were also used for below real-time PCR, were obtained from Applied Biosystems, Inc. PCR products (10 μL) were loaded on 2.5% agarose gel containing ethidium bromide.

Real-time RT-PCR was used to analyze the expression of various apoptosis-related genes. Oligonucleotide primers and Taqman probes specific for p53 (tumor suppressor protein), p21 [cyclin-dependent kinase (CDK) inhibitor 1A, a cell cycle inhibitory gene protein], GADD45α (growth arrest and DNA damage–inducible protein, α), and CCND1 (cyclin D1) were obtained from Applied Biosystems. mRNA expression was analyzed via quantitative real-time RT-PCR as detailed by us previously (34). Isolation of total RNA was done as described above. Purified RNA (25 ng) was used to do RT-PCR in an Applied Biosystems Prism 7000 Sequence Detection System, with the use of One-Step RT-PCR Master Mix Reagents. Data were normalized to GAPDH mRNA.

Western Blot Analysis

Western immunoblots were run as described previously (35). Primary antibodies and their sources were as follows. Anti–total p38 MAPK, anti–total p53, anti–phosphorylated p53 (pp53), and anti–activated caspase 3 were from Cell Signaling Technology. Anti–phosphorylated p38 (pp38) MAPK was from Millipore. Anti-p21 was from Abcam. Anti–β-actin and the secondary antibodies horseradish peroxidase–conjugated anti-rabbit IgG and anti-rabbit IgG were from Sigma-Aldrich. Anti-goat IgG was from Santa Cruz Biotechnology.

Data Analysis

For all experiments, viral transduction was done in triplicate wells and repeated at least thrice. Data are expressed as mean ± SE of three or more independent determinations. Statistical significance was evaluated with the use of a one- or two-way ANOVA as appropriate followed by a post hoc test (Bonferroni) to compare individual means. Differences were considered significant at $P < 0.05$.

Results

Endogenous and Adenoviral-Mediated Expression of AT2R in Prostate Cancer Cells

The presence of endogenous AT2R within human prostate cancer cell lines was first assessed using RT-PCR. Initial analyses using 35 cycles of PCR failed to reveal AT2R mRNA in untreated DU145, PC3, or LNCaP cells. However, further analyses using 40 cycles of PCR revealed AT2R transcripts in DU145 and PC3 cells, but not in LNCaP cells (Fig. 1, *top*). In addition, DU145 cells infected with Ad-CMV-EGFP (100 ifu/cell, 2 days) exhibited no AT2R immunoreactivity (Fig. 1, *middle*), consistent with a previous report (36). Collectively, these results indicate that endogenous AT2Rs are present in the cell lines tested, in particular the DU145 cells, at only low levels.

Our previous studies using real-time RT-PCR or AT2R binding assays showed that Ad-G-AT2R-EGFP elicited significant expression of AT2R within various cell lines (e.g., C2C12 mouse muscle myoblasts, NIH/3T3 fibroblasts, and CATH.a locus ceruleus tumor cells; ref. 33) and in primary cultures of neonatal rat cardiac fibroblasts (37). Ad-G-AT2R-EGFP also proved to be effective in eliciting AT2R expression in human prostate cancer cells. The fluorescence micrographs presented in Fig. 1 (*bottom*) show that incubation of DU145 prostate cancer cells with Ad-G-AT2R-EGFP (100 ifu/cell) produced a high level of expression of AT2R immunoreactivity and GFP at 48 hours after viral transduction when compared with DU145 cells that had been infected with Ad-CMV-EGFP (Fig. 1, *middle*). Similar results were obtained following Ad-G-AT2R-EGFP infection of LNCaP and PC3 human prostate cancer cells and WPMY-1 normal human prostate cells (data not shown).

Effect of Increased AT2R Expression on Cell Cycle Progression and Cell Proliferation in DU145 Cells

Analysis via flow cytometry of the cell cycle distribution of DU145 cells revealed that transduction with Ad-G-AT2R-EGFP (100 ifu/cell, 24 hours) produced a significant reduction in the number of S-phase cells and an increase in G_1-phase cells when compared with cells transduced with Ad-CMV-EGFP (100 ifu/cell, 24 hours). Neither vector produced significant changes in the level of G_2 cells present in DU145 cells nor in the numbers of G_1, S, and G_2 cells present in normal human prostate WPMY-1 cells (Fig. 2A and B). Similar transduction of DU145 cells with Ad-G-AT2R-EGFP also significantly inhibited their proliferation, an effect that was not observed in WPMY-1 cells (Fig. 2C).

AT2R Overexpression Induces Apoptosis in Prostate Cancer Cells

Transduction of DU145 cells with Ad-G-AT2R-EGFP (100 ifu/cell) for 2 days resulted in a large number of cells that exhibited apoptotic-like morphologic characteristics when compared with Ad-CMV-EGFP–treated DU145 cells (Figs. 1, *bottom*, and 3A; Supplementary Fig. S1). For

Published OnlineFirst December 8, 2009; DOI: 10.1158/1535-7163.MCT-09-0237

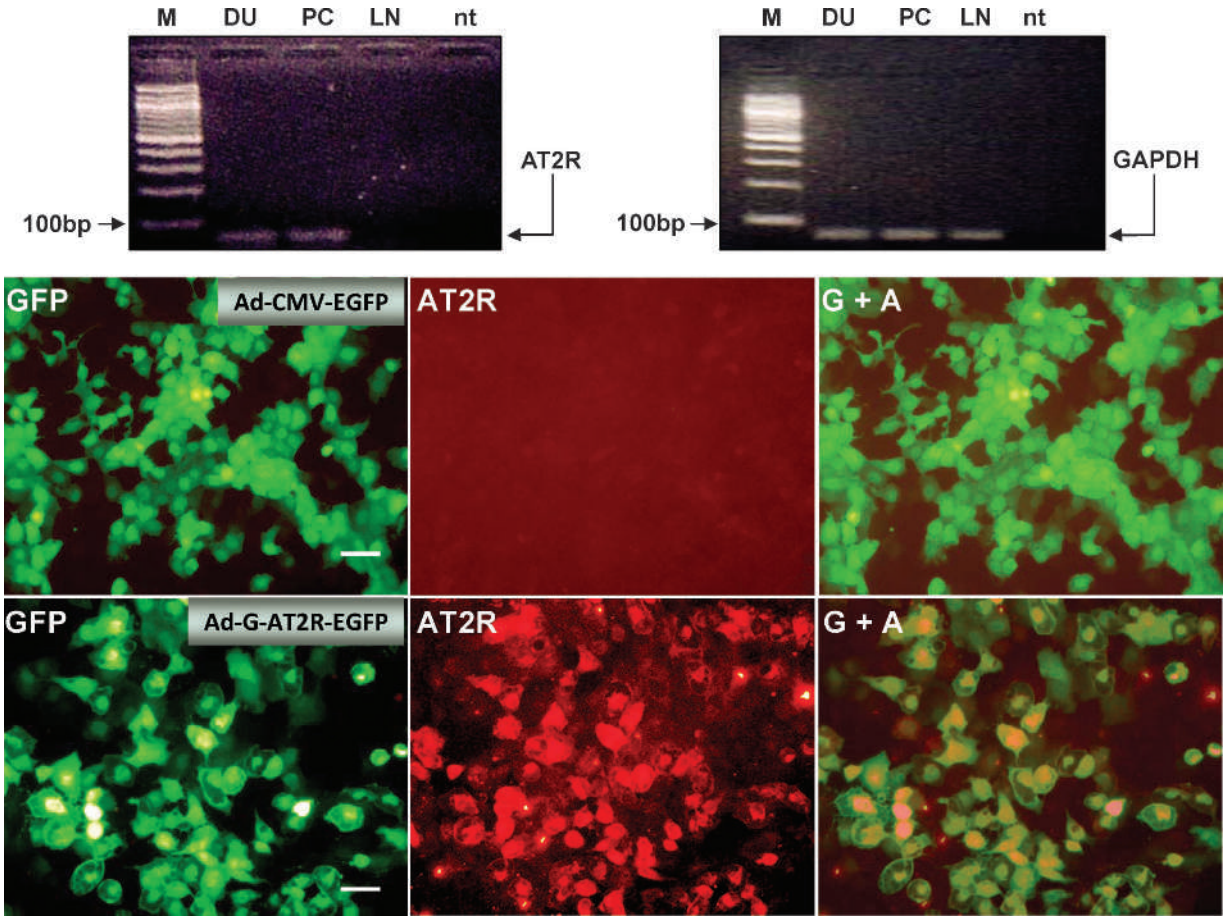

Figure 1. Basal and viral vector–mediated expression of AT2R in prostate cancer cell lines. *Top,* total RNA was extracted from untreated prostate cancer cell lines (DU145, PC3, and LNCaP) and AT2Rs were detected by RT-PCR. Ethidium bromide–stained gels show AT2R (*left*) and GAPDH (*right*) transcripts in each cell type. *M,* 100-bp ladder (New England Biolabs); *DU,* DU145 cells; *PC,* PC3 cells; *LN,* LNCaP cells; *nt,* no template control. *Bottom,* DU145 cells were transduced with either Ad-CMV-EGFP or Ad-G-AT2R-EGFP (100 ifu/cell) for 2 d as described in Materials and Methods. Incubations were followed by detection of EGFP fluorescence and AT2R immunoreactivity using an anti-AT2R antibody. Representative fluorescence micrographs from Ad-CMV-EGFP–transduced and Ad-G-AT2R-EGFP–transduced cells, showing EGFP fluorescence, AT2R immunostaining, and merged (*G + A*) EGFP/AT2R in each treatment condition. *Scale bars,* 50 μm.

example, the AT2R-expressing DU145 cells exhibited irregular-shaped nuclei and a clear boundary between nuclei and cytoplasm when compared with the controls (Supplementary Fig. S1). Similar transduction of LNCaP and PC3 cells with Ad-G-AT2R-EGFP also resulted in the appearance of cells with apoptotic-like morphology, although the effect in PC3 cells was much weaker than that observed in DU145 or LNCaP cells (Fig. 3A). Because this effect of AT2R is significant and easily recognizable in DU145 cells, our subsequent experiments were focused mostly on this tumor cell line. The apoptotic action following AT2R transduction was confirmed by the finding that incubation of DU145 cells with Ad-G-AT2R-EGFP (100 ifu/cell) for 2 days produced a significant increase in TUNEL labeling compared with the Ad-CMV-EGFP (100 ifu/cell)–treated cells (Fig. 3B and C). In contrast to the prostate cancer cells, WPMY-1 cells transduced with Ad-G-AT2R-EGFP (100 ifu/cell) for 2 days exhibited no significant morphologic changes compared with Ad-CMV-EGFP–transduced WPMY-1 cells (Supplementary Fig. S1). Consistent with these findings, transduction of Ad-G-AT2R-EGFP into DU145 cultures resulted in significant cytotoxicity, whereas no such cytotoxic action was observed in WPMY-1 cells. Specifically, DU145 cultures exhibited 22.2 ± 1.9% cell death ($n = 3$ experiments) following Ad-G-AT2R-EGFP transduction compared with 3.7 ± 0.8% cell death ($n = 3$ experiments) in Ad-CMV-EGFP–transduced cultures. In comparison, the levels of cell death in Ad-G-AT2R-EGFP–transduced and Ad-CMV-EGFP–transduced WPMY-1 cultures were 0.7 ± 0.2% and 2.3 ± 0.6%, respectively ($n = 3$ experiments).

Apoptosis Induced by AT2R Overexpression Is Not Dependent on Ang II

Considering that Ang II has been shown to have antigrowth effects in DU145 cells (24), we tested whether the apoptosis produced by overexpression of AT2R was Ang II dependent. Apoptosis was assessed by measuring the

Published OnlineFirst December 8, 2009; DOI: 10.1158/1535-7163.MCT-09-0237

number of green fluorescing cells that exhibit apoptotic morphology. The data presented in Fig. 3D indicate that neither Ang II (1 μmol/L) nor the AT2R partial agonist CGP42112A (1 μmol/L) affects the number of apoptotic cells present following overexpression of AT2R via Ad-G-AT2R-EGFP. Likewise, the AT2R-mediated increase in apoptosis was not significantly altered by the AT2R- or AT1R-selective antagonists PD123319 (10 μmol/L) and losartan (10 μmol/L), either alone or in combination with Ang II ($P > 0.1$), although there is a tendency for apoptosis to decrease in the cells treated with PD123319 or PD123319 plus Ang II (Fig. 3D). In addition, treatment of cells with the nonselective Ang II receptor blocker saralasin (10 μmol/L) did not alter the AT2R-induced apoptosis (Fig. 3D). None of these treatments produced significant levels of apoptosis in the Ad-CMV-EGFP–transduced DU145 cells (Fig. 3D),

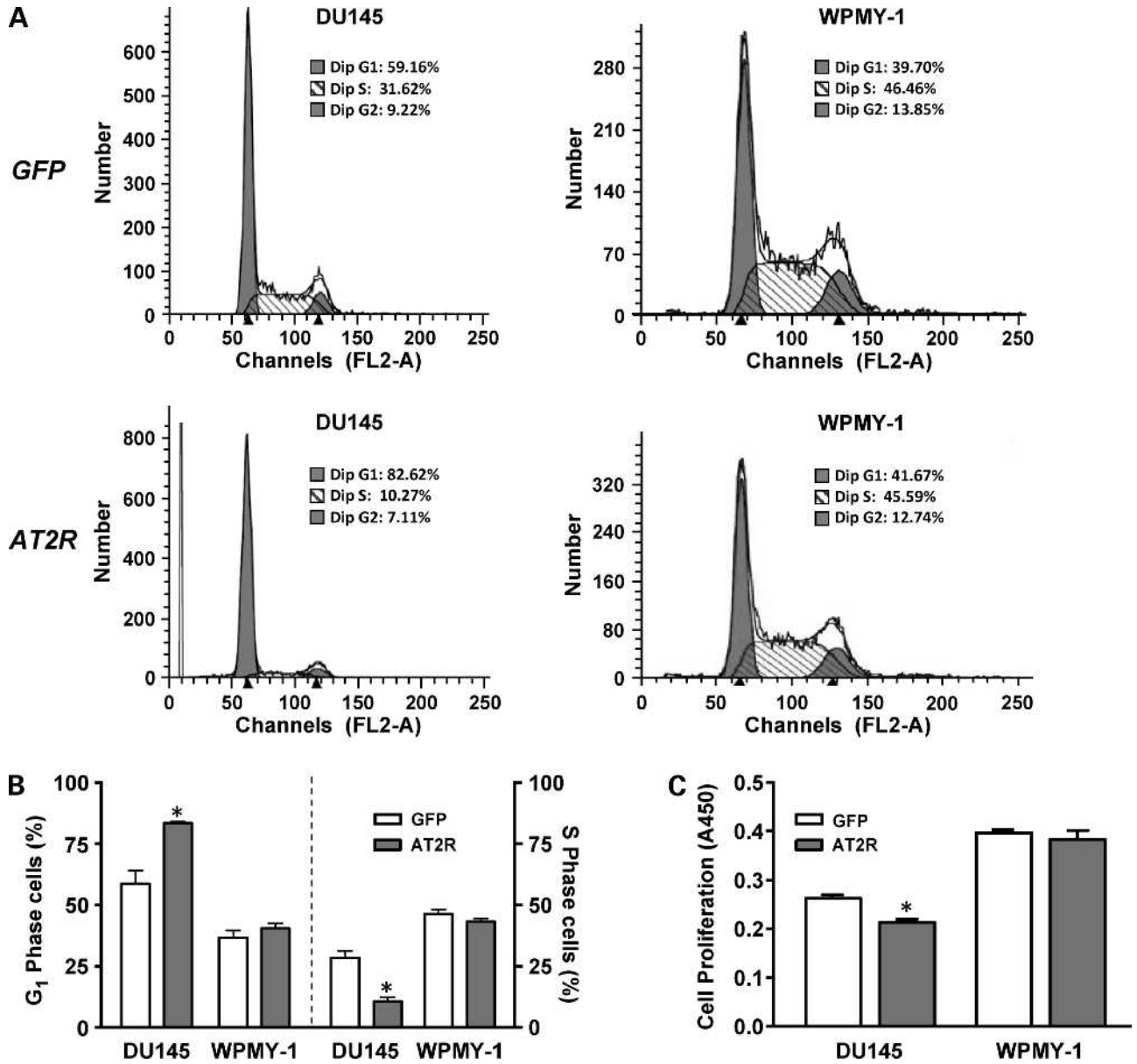

Figure 2. Increased expression of AT2R in DU145 cells: effects on cell cycle and proliferation. **A,** DU145 or WPMY-1 cells were transduced with 100 ifu/cell of either Ad-G-AT2R-EGFP or Ad-CMV-EGFP for 24 h and then fixed, permeabilized with ethanol, and stained with propidium iodide as described in Materials and Methods. Fluorescence intensity was measured by flow cytometry. Representative histograms show the DNA contents during G_1, S, and G_2 phases under each treatment condition. **B,** data showing percentages of DU145 and WPMY-1 cells in G_1 phase (*left*) and S phase (*right*) under each treatment condition. *Columns,* mean ($n = 3$); *bars,* SE. Data are derived from DNA histograms. *, $P < 0.01$ versus Ad-CMV-EGFP–transduced cells. **C,** DU145 or WPMY-1 cells underwent transduction with either Ad-CMV-EGFP or Ad-G-AT2R-EGFP (100 ifu/cell) for 24 h. Following this, WST-1 reagent was added to the culture medium (1:10 dilution), and absorbance was measured at 450 nm. *Columns,* mean A_{450} nm from three experiments; *bars,* SE. *, $P < 0.01$ versus Ad-CMV-EGFP–transduced cells.

Published OnlineFirst December 8, 2009; DOI: 10.1158/1535-7163.MCT-09-0237

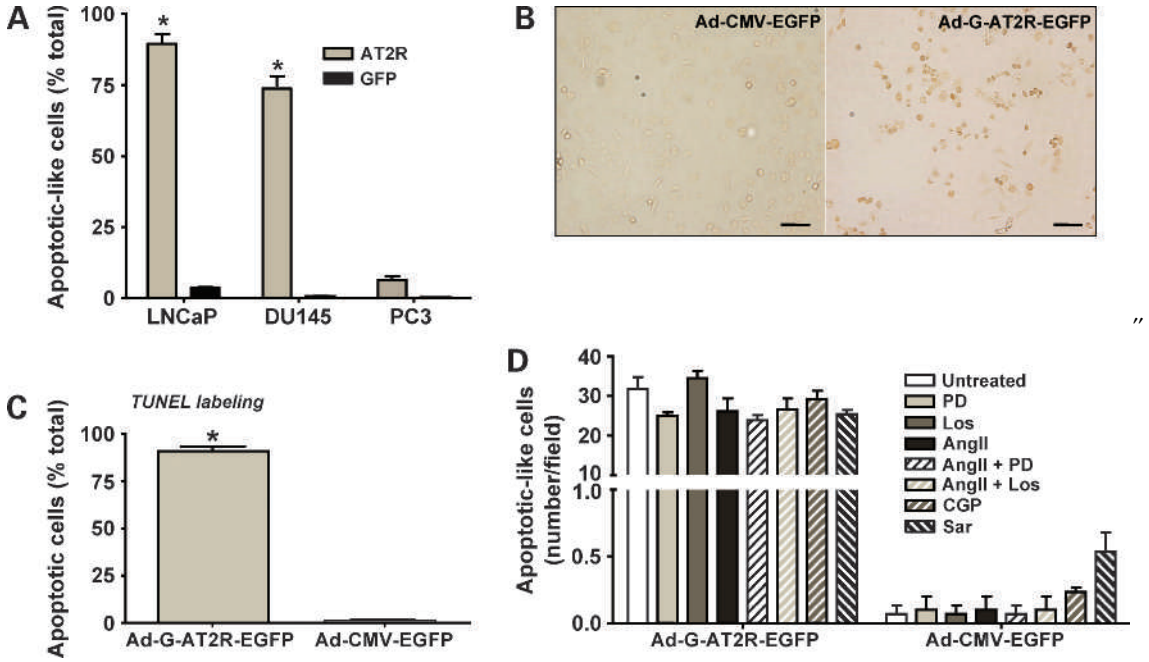

Figure 3. AT2R-induced apoptosis of DU145 prostate cancer cells. **A,** DU145, LNCaP, or PC3 cells were transduced with either Ad-CMV-EGFP or Ad-G-AT2R-EGFP (100 ifu/cell) for 2 d as described in Materials and Methods. Incubations were followed by detection of EGFP fluorescence and counting of cells that display apoptotic-like morphology from 10 random fields per well. Numbers of apoptotic cells are expressed as a percent of the total cells in the dish. *Columns,* mean from three separate experiments; *bars,* SE. *, $P < 0.001$ versus corresponding GFP-transduced cells. **B,** DU145 cells were transduced with either Ad-CMV-EGFP or Ad-G-AT2R-EGFP (100 ifu/cell) for 2 d, and apoptotic cells were detected using the DeadEnd Colorimetric TUNEL System kit. Two representative phase-contrast micrographs from each treatment condition. The brown-colored nuclei represent TUNEL-positive (apoptotic) cells. **C,** quantification of the TUNEL-positive cells as a percent of the total number of cells in the dish. *Columns,* mean of three experiments; *bars,* SE. *, $P < 0.001$ versus GFP group. **D,** DU145 cells were transduced with Ad-G-AT2R-EGFP or Ad-CMV-EGFP (100 ifu/cell) for 6 h and then treated with Ang II (1 μmol/L) or Ang II receptor agonists/antagonists as described in Materials and Methods. *PD,* PD123319 (10 μmol/L); *Los,* losartan (10 μmol/L); *Sar,* saralasin (10 μmol/L); *CGP,* CGP42112A (1 μmol/L). At 48 h after vector treatment, apoptosis was assessed by counting the cells with apoptotic-like morphology from 10 random fields per well. *Columns,* mean from three separate experiments; *bars,* SE.

suggesting that the low levels of endogenous AT2R present in DU145 are not functional in terms of apoptosis. Collectively, these data suggest that the apoptosis induced by AT2R overexpression in DU145 cells is Ang II independent and AT2R itself has constitutive activity to cause apoptosis.

AT2R-Induced Apoptosis Is Mediated by p38 MAPK and Caspase-3 via an Extrinsic Cell Death Signaling Pathway

Immunoblot analysis indicated that a ~43-kDa protein that cross-reacts with a specific antibody against activated p38 MAPK (pp38) is present in DU145 cells (Fig. 4A). The blot also revealed that in the Ad-G-AT2R-EGFP–transduced cells, basal levels of pp38 MAPK were elevated in a dose-independent manner when compared with Ad-CMV-EGFP–transduced or mock-transduced (control) DU145 cells. Basal levels of total p38 MAPK were not changed under these treatment conditions (Fig. 4A). Treatment of DU145 cells with the p38 MAPK inhibitor SB203580 (10 μmol/L; 6 hours after viral transduction) decreased pp38 MAPK levels but did not alter total p38 MAPK levels in the AT2R-transduced cells (Fig. 4B, *left*). This treatment also caused a significant reduction (~68%) in the apoptosis induced by AT2R overexpression (Fig. 4B, *right*). DU145 cells treated with the control vector Ad-CMV-EGFP display only low levels of apoptosis (Fig. 3), and treatment of Ad-CMV-EGFP–transduced cells with SB203580 as above did not alter the level of apoptosis (data not shown). In a different approach, we tested the effects of knockdown of p38, using p38 siRNA, on the AT2R-induced apoptosis. Transfection of p38 MAPK siRNA into DU145 cells reduced the levels of both p38 MAPK and pp38 MAPK (Fig. 4C, *left*) and caused a significant (~77%) reduction in the AT2R-induced apoptosis (Fig. 4C, *right*). These results suggest a significant functional role for p38 MAPK in the AT2R-mediated apoptotic action in DU145 cells. The activation of class II caspases is considered a hallmark of programmed cell death (38). For example, caspase-8 is required for the initiation phase of the extrinsic cell death signaling pathway, whereas activation of caspase-9 is integral to the intrinsic cell death pathway that involves mitochondrial release of cytochrome *c* (39). All initiator caspase activation leads to the eventual proteolytic activation of the effector caspase-3, which cleaves large numbers of cellular proteins leading to apoptosis. Thus, we first examined the role of caspase-3 in apoptosis induced by overexpression of AT2R. Cell-free extracts prepared from Ad-G-AT2R-EGFP (100 ifu/cell)–transduced DU145 cells displayed significantly higher

Published OnlineFirst December 8, 2009; DOI: 10.1158/1535-7163.MCT-09-0237

caspase-3–like activity compared with extracts from Ad-CMV-EGFP (100 ifu/cell)–transduced cells or mock-transduced cells (Fig. 5A). Further, transduction of LNCaP cells with Ad-G-AT2R-EGFP (20 or 100 ifu/cell) resulted in cleavage of the ~32-kDa caspase-3 protein to yield the active ~17- and 19-kDa subunits as seen by Western blot analysis (Fig. 5B). No such proteolytic processing of caspase-3 was seen in the Ad-CMV-EGFP–transduced or in the mock-transduced (control) LNCaP cells (Fig. 5B). Lastly, treatment of DU145 cells with the caspase-3 inhibitor Ac-DEVD-CMK (20 μmol/L) significantly reduced the apoptosis elicited by transduction with 100 ifu/cell Ad-G-AT2R-EGFP (Fig. 5C). Interestingly, similar inhibition of AT2R-induced apoptosis was obtained by treatment of the DU145 cells with the caspase-8 inhibitor Z-IETD-FMK (20 μmol/L), but the caspase-9 inhibitor Z-LEHD-FMK (20 μmol/L) was without effect (Fig. 5C). Collectively, these data suggest the involvement of a caspase-8–mediated extrinsic signaling pathway followed by downstream activation of caspase-3 in the apoptosis elicited by overexpression of AT2R in prostate cancer cells.

AT2R Overexpression-Induced Changes in Gene Expression in DU145 Cells

Considering the significant apoptotic action produced by overexpression of AT2R in prostate cancer cell lines, we next explored the effects of increased expression of AT2R on genes related to apoptosis and the cell cycle. As shown in Fig. 6A, in DU145 cells transduced with Ad-G-AT2R-EGFP (100 ifu/cell), there was no significant change in the levels of mRNA of p53 (a tumor suppressor protein), but the level of activated p53 (pp53) was enhanced when compared with levels in Ad-CMV-EGFP–transduced or mock-transduced (control) cells (Fig. 6B). AT2R overexpression in DU145 cells also produced the following

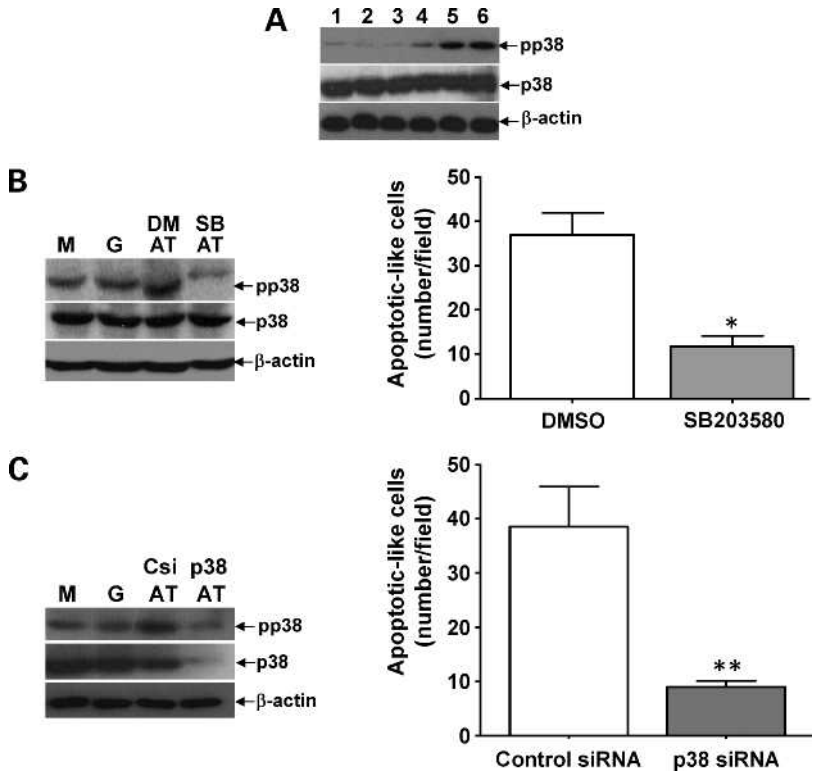

Figure 4. Involvement of p38 MAPK in AT2R-mediated apoptosis in DU145 prostate cancer cells. **A,** representative Western blots showing the p38 MAPK and pp38 MAPK in DU145 cells under the following treatment conditions. *Lane 1,* mock viral transduction; *lanes 2* and *3,* transduction for 2 d with Ad-CMV-EGFP (50 and 100 ifu/cell, respectively); *lanes 4, 5,* and *6,* transduction for 2 d with Ad-G-AT2R-EGFP (50, 100, and 200 ifu/cell, respectively). Data are representative of three experiments. **B,** *left,* representative Western blots showing p38 MAPK and pp38 MAPK in transduced DU145 cells following treatment with the p38 MAPK inhibitor SB203580. *M,* mock viral transduction; *G,* transduction for 2 d with Ad-CMV-EGFP (100 ifu/cell); *AT,* Ad-G-AT2R-EGFP (100 ifu/cell) transduction for 2 d plus treatment with DMSO (*DM*) or SB203580 (*SB*). Data are representative of three experiments. *Right,* DU145 cells were transduced with Ad-G-AT2R-EGFP (100 ifu/cell) for 6 h followed by treatment with either the p38 MAPK inhibitor SB203580 (10 μmol/L) or control solvent (*DMSO*) for 24 h. Green fluorescent cells exhibiting apoptotic morphology were counted from 10 fields per well. *Columns,* mean of three experiments; *bars,* SE. *, $P < 0.01$ versus control (DMSO-treated) cells. **C,** *left,* representative Western blots showing p38 MAPK and pp38 MAPK in transduced DU145 cells following treatment with the p38 siRNA or the control siRNA. *AT,* Ad-G-AT2R-EGFP (100 ifu/cell) transduction for 2 d plus treatment with p38 siRNA (*p38*) or the control siRNA (*Csi*). Data are representative of three experiments. *Right,* DU145 cells were transfected with p38 siRNA (20 nmol/L) or control siRNA (20 nmol/L) followed by transduction with Ad-G-AT2R-EGFP (100 ifu/cell) for 2 d. Green fluorescent cells exhibiting apoptotic morphology were counted from 10 fields per well. *Columns,* mean of three experiments; *bars,* SE. *, $P < 0.001$ versus control siRNA–transfected cells.

Published OnlineFirst December 8, 2009; DOI: 10.1158/1535-7163.MCT-09-0237

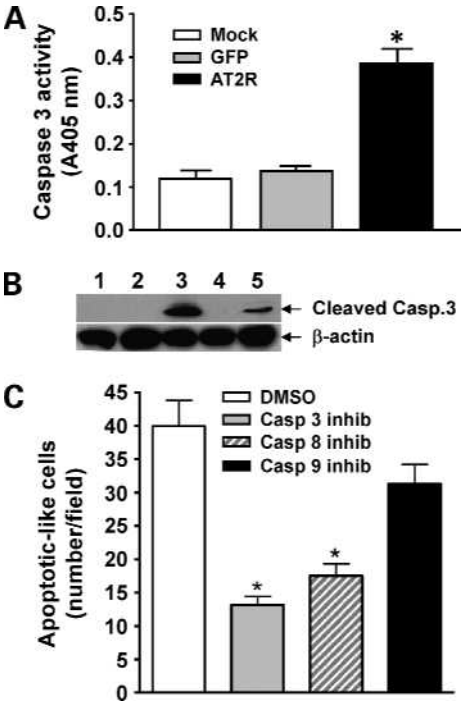

Figure 5. Role of caspases in AT2R-induced apoptosis in prostate cancer cells. **A,** AT2R-induced increase in caspase-3 activity in DU145 cells. Cells underwent transduction with Ad-CMV-EGFP or Ad-G-AT2R-EGFP (100 ifu/cell) or were mock transduced for 2 d. Following this, cells were washed and lysed, and total cellular protein was assayed for caspase-3–like activity by measuring the release of pNA from the colorimetric caspase-3 substrate z-DEVD-pNA. *Columns,* mean A_{405} nm from three experiments; *bars,* SE. *, $P < 0.01$ versus Ad-CMV-EGFP–transduced or mock-transduced cells. **B,** AT2R-induced increase in cleaved caspase-3 generation in LNCaP cells. Cells were infected with either 20 or 100 ifu/cell of Ad-CMV-EGFP (*lanes 2* and *4*, respectively) or 20 or 100 ifu/cell of Ad-G-AT2R-EGFP (*lanes 3* and *5*, respectively) or were mock transduced (*lane 1*). At 48 h after transduction, cell protein extracts were subjected to Western blot analysis. Representative blots (representative of three different experiments) indicating cleaved caspase-3 protein bands (17 and 19 kDa) and β-actin under each treatment condition. **C,** effects of caspase inhibitors on AT2R-mediated apoptosis in DU145 cells. Cells were transduced with Ad-G-AT2R-EGFP (100 ifu/cell) for 6 h followed by treatment with either the caspase-3 inhibitor Ac-DEVD-CMK (20 μmol/L), the caspase-8 inhibitor Z-IETD-FMK (20 μmol/L), the caspase-9 inhibitor Z-LEHD-FMK (20 μmol/L), or control solvent (DMSO) for 24 h. Green fluorescent cells exhibiting apoptotic morphology were counted from 10 fields per well. *Columns,* mean of three experiments; *bars,* SE. *, $P < 0.01$ versus control (DMSO-treated) cells.

changes in gene and/or protein expression. The expression of mRNA for *p21*, the most prominent p53-regulatory gene, was markedly increased in cells transduced with Ad-G-AT2R-EGFP in a dose-dependent manner (Fig. 6A). A similar effect on p21 protein was also observed in Ad-G-AT2R-EGFP–treated cells (Fig. 6B). The mRNA for *GADD45α*, a p53-dependent gene, was also dramatically induced (Fig. 6A), whereas expression of mRNA for *CCND1*, a key cell cycle regulator of the G_1- to S-phase transition, was significantly decreased (Fig. 6A). To explore the respective roles of p53 and p21 in the AT2R-induced increase in apoptosis, we tested the effects of p53 siRNA and p21 siRNA on the apoptosis produced by transduction of DU145 cells with Ad-G-AT2R-EGFP. Transfection of p53 and p21 siRNA into DU145 cells produced respective decreases in p53 and p21 expression (Fig. 6C). Treatment of DU145 cells with the p53 siRNA significantly blocked the AT2R-induced apoptosis by ~39% (Fig. 6D). However, knockdown of p21 expression had no significant effect on the level of apoptosis elicited by AT2R overexpression (Fig. 6D). It is also noteworthy that in PC3 cells, which are devoid of p53, the level of AT2R-induced apoptosis was weak when compared with the effects in DU145 or LNCaP cells (Fig. 3C; Supplementary Fig. S1). Collectively, these data indicate that the apoptosis induced by AT2R overexpression is at least partially dependent on p53 Ser^{15} phosphorylation, but not on p21.

Discussion

In this study, we first showed that certain prostate cancer cell lines (DU145 and PC3) exhibit only low levels of endogenous AT2R and that, in LNCaP prostate cancer cells, levels of this angiotensin receptor subtype were below detection. Further, activation of these endogenous AT2Rs in control DU145 cells by Ang II or an AT2R-selective agonist failed to induce apoptosis. In contrast, Ad-G-AT2R-EGFP–induced overexpression of AT2R in all three prostate cancer cell lines produced apoptosis. This apoptotic effect was dramatic in the p53-expressing DU145 cells and LNCaP cells but was much weaker in PC3 cells that do not express p53. Interestingly, the apoptotic effect of increased AT2R expression did not require Ang II. The data presented here indicate that AT2R overexpression in DU145 cells induced inhibition of proliferation, a significant reduction of S-phase cells, and an enrichment of G_1-phase cells. Furthermore, the data also indicate that overexpression of AT2R led to apoptosis via an extrinsic cell death signaling pathway that is dependent on activation of p38 MAPK, caspase-8, and caspase-3. Finally, the apoptosis induced by AT2R overexpression is partially dependent on the activation of p53, but not on p21. This latter finding may partially explain the weak effects of AT2R overexpression on apoptosis in PC3 cells. Collectively, the observations presented here indicate the ability of increased AT2R expression to induce apoptosis in prostate cancer cell lines *in vitro*.

Although the studies presented here show an effective and potent action of AT2R to elicit apoptosis of prostate cancer cells *in vitro*, there are many issues raised and questions that remain to be answered. For example, an extrapolation of this study is that AT2R may be a promising novel target for prostate cancer gene therapy. There are several unique features of prostate cancer that make it particularly amenable to gene therapy approaches, including the availability of several prostate-specific promoters, which would allow tissue-specific expression of therapeutic gene products, and the relatively easy access to the prostate by transurethral, transperineal, and transrectal approaches (40). Thus, identification of a target such as AT2R that has powerful apoptotic actions in prostate tumor cells but not in normal prostate tissue may be an excellent candidate for prostate cancer gene therapy. However, before that step could occur, it will be

Published OnlineFirst December 8, 2009; DOI: 10.1158/1535-7163.MCT-09-0237

imperative to test the efficacy of AT2R gene transduction in animal models. Thus, certain of our future studies will be aimed at examining the ability of Ad-G-AT2R-EGFP to suppress prostate tumor growth *in vivo*. Along these lines, we are currently planning to test the effectiveness of this viral construct in eliciting apoptosis in nude mice DU145 xenografts. If effective, a further step would be to construct new AT2R adenoviral vectors containing prostate-specific promoters, such as the long prostate-specific antigen and osteocalcin promoters (10, 41). This may allow us to target metastatic prostate tumor cells, which is one major challenge and unresolved problem in prostate cancer gene therapy.

A further issue that warrants discussion is the mechanism of action of AT2R in promoting apoptosis of prostate cancer cells. Other studies have indicated that AT2R-mediated apoptosis seems to involve different mechanisms depending on the cell type. For example, in several cell culture models, it has been shown that Ang II is capable of inhibiting growth and inducing apoptosis via endogenous AT2R (17, 32). This antigrowth action is mediated by downregulation of p42/p44 MAPK, and apoptosis is considered to be an extreme result of inhibition of antigrowth signaling. However, it is also apparent that in certain cell types, activation of AT2R by Ang II is not required to elicit apoptosis, as apoptotic cell death induced by AT2R overexpression in R3T3 fibroblasts, Chinese hamster ovary epithelial cells, and A7r5 vascular smooth muscles cells could only be blocked by mutation of the receptor or pharmacologic inhibition of signaling intermediates (i.e., p38 MAPK inhibition and caspase-3 inhibition; ref. 29). Consistent with this study, our experiments indicate that AT2R overexpression-induced apoptosis is ligand (Ang II) independent, is mediated by p38 MAPK and caspase-3, and, in addition, occurs via an extrinsic cell death signaling pathway. One interesting question that remains is whether agents that can increase the expression of endogenous AT2R in prostate cancer cells have the ability to induce apoptosis.

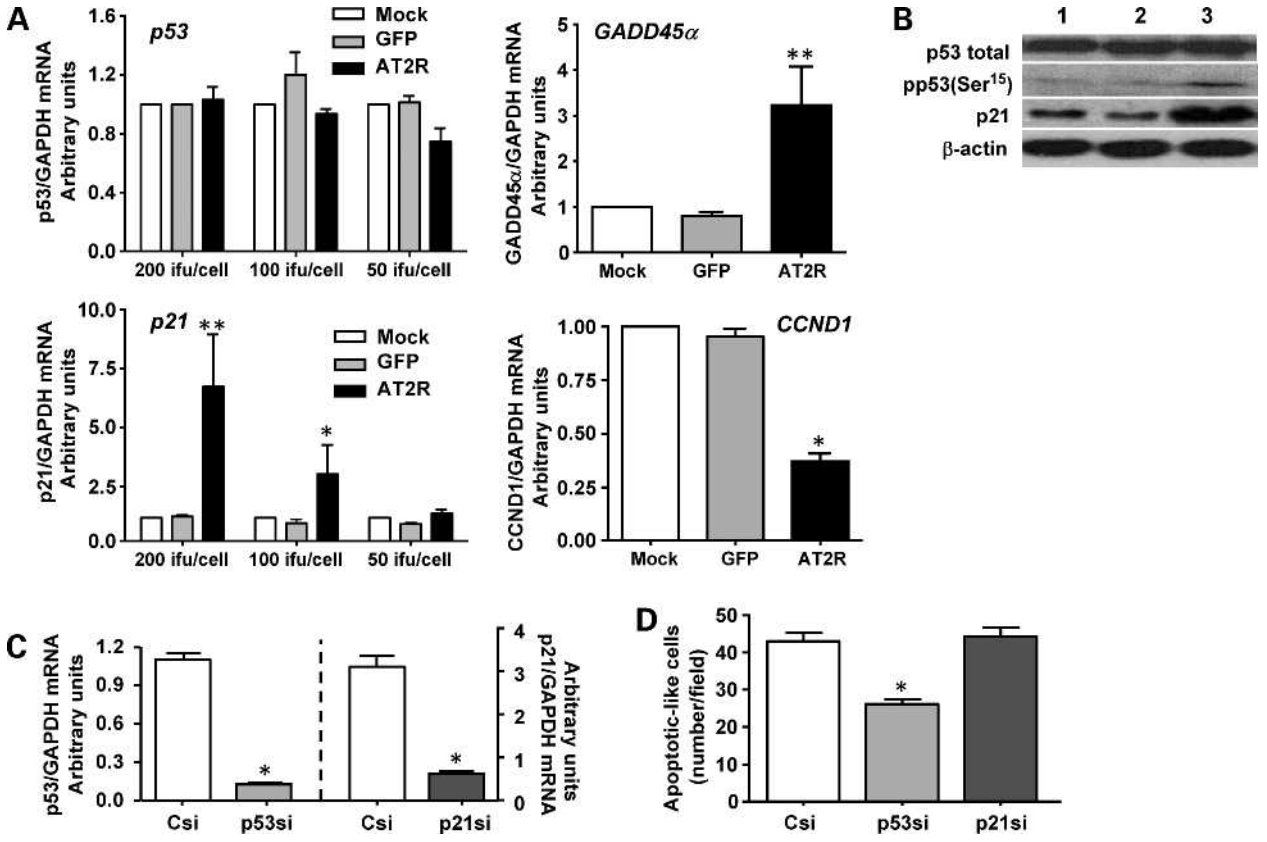

Figure 6. Role of apoptosis-associated genes in AT2R-induced apoptosis in DU145 cells. **A,** DU145 cells were transduced with either Ad-G-AT2R-EGFP (AT2R) or Ad-CMV-EGFP (GFP) for 2 d at the indicated doses (*p53* and *p21 panels*) or at 100 ifu/cell (*GADD45α* and *CCND1 panels*). Other groups of cells were mock transduced. These treatments were followed by isolation of mRNA and then real-time RT-PCR analysis of either p53, p21, GADD45α, or CCND1 using specific oligonucleotide primers and Taqman probes. All data were normalized against levels of GAPDH mRNA expression within the same sample. *Columns,* mean from three separate experiments; *bars,* SE. **, $P < 0.01$; *, $P < 0.05$ versus Ad-CMV-EGFP–transduced or mock-transduced cells. **B,** DU145 cells were transduced with either 100 ifu/cell of Ad-CMV-EGFP or Ad-G-AT2R-EGFP or were mock transduced. After 2 d of incubation, cells were collected and subjected to Western blot analyses. Blots (representative of three different experiments) indicating total p53, pp53, p21, and β-actin protein bands in mock-transduced (*lane 1*), Ad-CMV-EGFP–transduced (*lane 2*), or Ad-G-AT2R-EGFP–transduced (*lane 3*) cells. **C** and **D,** DU145 cells were treated with 20 nmol/L of either p53 siRNA (*p53si*), p21 siRNA (*p21si*), or control siRNA and Ad-G-AT2R-EGFP (100 ifu/cell) as described in Materials and Methods followed 48 h later by real-time RT-PCR analysis (**C**) of either p53 mRNA (*left*) or p21 mRNA (*right*) or assessment of cells with apoptotic-like morphology (**D**). *Columns,* mean from three separate experiments in each case; *bars,* SE. *, $P < 0.01$ versus control siRNA–transfected cells.

Published OnlineFirst December 8, 2009; DOI: 10.1158/1535-7163.MCT-09-0237

The data presented here also indicate that p53 is involved in the AT2R-mediated apoptosis of DU145 cells. This tumor suppressor gene plays an important role during the induction of apoptosis. Androgen-independent DU145 cells have a mutated p53 gene, and the expression of androgen receptors is inhibited by promoter methylation (42, 43). It was observed that the mutant p53 can be phosphorylated on various sites *in vitro* and in human tumors *in vivo*. Ser^{15} or Ser^{315} phosphorylation tends to restore wild-type function in the mutated proteins. It is possible that phosphorylation of serine residues in addition to residue 15 can lead to an increase of p53 stability, DNA binding, and gain of function and contribute to apoptosis (44). In the present study, we have shown that AT2R overexpression increases the phosphorylation of p53 at Ser^{15} in DU145 cells and also increases the expression of the p53-dependent genes *p21* and *GADD45α*. *p21* binds to and inhibits the activity of cyclin-CDK2 or cyclin-CDK4 complexes and thus functions as a regulator of cell cycle progression at G_1. Our experiments indicate that apoptosis induced by AT2R overexpression is partially dependent on p53 Ser^{15} phosphorylation in DU145 cells, but increased expression of p21 does not seem to contribute directly to the apoptosis (Fig. 6).

In summary, we have made the novel observation that overexpression of AT2R in prostate cancer cell lines results in a powerful apoptotic action. The therapeutic value of this observation remains to be assessed, but the fact that similar overexpression of AT2R in normal prostate cells does not elicit apoptotic cell death suggests that the strategy of targeting this angiotensin receptor subtype in prostate cancer may be promising.

Disclosure of Potential Conflicts of Interest

No potential conflicts of interest were disclosed.

Acknowledgments

We thank Dr. Howard Johnson (University of Florida) for providing the PC3 cell line used in this study and Drs. Nan Jiang, Peng Shi, Zhiying Shan, and Neal Benson (all University of Florida) for technical assistance.

References

1. Jemal A, Siegel R, Ward E, et al. Cancer statistics, 2008. CA Cancer J Clin 2008;58:71–96.

2. Jemal A, Thun MJ, Ries LA, et al. Annual report to the nation on the status of cancer, 1975-2005, featuring trends in lung cancer, tobacco use, and tobacco control. J Natl Cancer Inst 2008;100:1672–94.

3. Dijkman GA, Van Moorselaar RJ, Van Ginckel R, et al. Antitumoral effects of liarozole in androgen-dependent and independent R3327-Dunning prostate adenocarcinomas. J Urol 1994;151:217–22.

4. Freytag SO, Stricker H, Movsas B, Kim JH. Prostate cancer gene therapy clinical trials. Mol Ther 2007;15:1042–52.

5. Belldegrun A, Tso CL, Zisman A, et al. Interleukin 2 gene therapy for prostate cancer: phase I clinical trial and basic biology. Hum Gene Ther 2001;12:883–92.

6. Eder JP, Kantoff PW, Roper K, et al. A phase I trial of a recombinant vaccinia virus expressing prostate-specific antigen in advanced prostate cancer. Clin Cancer Res 2000;6:1632–38.

7. Freytag SO, Khil M, Stricker H, et al. Phase I study of replication-competent adenovirus-mediated double suicide gene therapy for the treatment of locally recurrent prostate cancer. Cancer Res 2002;62:4968–76.

8. Herman JR, Adler HL, Aguilar-Cordova E, et al. *In situ* gene therapy for adenocarcinoma of the prostate: a phase I clinical trial. Hum Gene Ther 1999;10:1239–49.

9. Kubo H, Gardner TA, Wada Y, et al. Phase I dose escalation clinical trial of adenovirus vector carrying osteocalcin promoter-driven herpes simplex virus thymidine kinase in localized and metastatic hormone-refractory prostate cancer. Hum Gene Ther 2003;14:227–41.

10. Shirakawa T, Terao S, Hinata N, et al. Long-term outcome of phase I/II clinical trial of Ad-OC-TK/VAL gene therapy for hormone-refractory metastatic prostate cancer. Hum Gene Ther 2007;18:1225–32.

11. Deshayes F, Nahmias C. Angiotensin receptors: a new role in cancer? Trends Endocrinol Metab 2005;16:293–99.

12. Uemura H, Ishiguro H, Kubota Y. Angiotensin II receptor blocker: possibility of antitumor agent for prostate cancer. Mini Rev Med Chem 2006;6:835–44.

13. Uemura H, Ishiguro H, Kubota Y. Pharmacology and new perspectives of angiotensin II receptor blocker in prostate cancer treatment. Int J Urol 2008;15:19–26.

14. Uemura H, Nakaigawa N, Ishiguro H, Kubota Y. Novel molecular targeting therapeutics for prostate cancer. Nippon Rinsho 2005;63:339–44.

15. Nakajima M, Hutchinson HG, Fujinaga M, et al. The angiotensin II type 2 (AT2) receptor antagonizes the growth effects of the AT1 receptor: gain-of-function study using gene transfer. Proc Natl Acad Sci U S A 1995;92:10663–67.

16. Timmermans PB, Smith RD. The diversified pharmacology of angiotensin II-receptor blockade. Blood Press Suppl 1996;2:53–61.

17. Stoll M, Steckelings UM, Paul M, Bottari SP, Metzger R, Unger T. The angiotensin AT2-receptor mediates inhibition of cell proliferation in coronary endothelial cells. J Clin Invest 1995;95:651–57.

18. Wolf G, Harendza S, Schroeder R, et al. Angiotensin II's antiproliferative effects mediated through AT2-receptors depend on down-regulation of SM-20. Lab Invest 2002;82:1305–17.

19. Meffert S, Stoll M, Steckelings UM, Bottari SP, Unger T. The angiotensin II AT2 receptor inhibits proliferation and promotes differentiation in PC12W cells. Mol Cell Endocrinol 1996;122:59–67.

20. Dinh DT, Frauman AG, Somers GR, et al. Evidence for activation of the renin-angiotensin system in the human prostate: increased angiotensin II and reduced AT(1) receptor expression in benign prostatic hyperplasia. J Pathol 2002;196:213–19.

21. Kosaka T, Miyajima A, Takayama E, et al. Angiotensin II type 1 receptor antagonist as an angiogenic inhibitor in prostate cancer. Prostate 2007;67:41–9.

22. Lawnicka H, Potocka AM, Juzala A, Fournie-Zaluski MC, Pawlikowski M. Angiotensin II and its fragments (angiotensins III and IV) decrease the growth of DU-145 prostate cancer *in vitro*. Med Sci Monit 2004;10:BR410–13.

23. Uemura H, Hasumi H, Ishiguro H, et al. Renin-angiotensin system is an important factor in hormone refractory prostate cancer. Prostate 2006;66:822–30.

24. Chow L, Rezmann L, Imamura K, et al. Functional angiotensin II type 2 receptors inhibit growth factor signaling in LNCaP and PC3 prostate cancer cell lines. Prostate 2008;68:651–60.

25. Bhaskaran M, Reddy K, Radhakrishanan N, Franki N, Ding G, Singhal PC. Angiotensin II induces apoptosis in renal proximal tubular cells. Am J Physiol Renal Physiol 2003;284:F955–65.

26. Cui TX, Nakagami H, Nahmias C, et al. Angiotensin II subtype 2 receptor activation inhibits insulin-induced phosphoinositide 3-kinase and Akt and induces apoptosis in PC12W cells. Mol Endocrinol 2002;16:2113–23.

27. Ding G, Reddy K, Kapasi AA, et al. Angiotensin II induces apoptosis in rat glomerular epithelial cells. Am J Physiol Renal Physiol 2002;283:F173–80.

28. Horiuchi M, Hayashida W, Kambe T, Yamada T, Dzau VJ. Angiotensin type 2 receptor dephosphorylates Bcl-2 by activating mitogen-activated protein kinase phosphatase-1 and induces apoptosis. J Biol Chem 1997;272:19022–26.

29. Miura S, Karnik SS. Ligand-independent signals from angiotensin II type 2 receptor induce apoptosis. EMBO J 2000;19:4026–35.

30. Miura S, Karnik SS, Saku K. Constitutively active homo-oligomeric angiotensin II type 2 receptor induces cell signaling independent of receptor conformation and ligand stimulation. J Biol Chem 2005;280:18237–44.

Published OnlineFirst December 8, 2009; DOI: 10.1158/1535-7163.MCT-09-0237

31. Shenoy UV, Richards EM, Huang XC, Sumners C. Angiotensin II type 2 receptor-mediated apoptosis of cultured neurons from newborn rat brain. Endocrinology 1999;140:500–09.

32. Yamada T, Horiuchi M, Dzau VJ. Angiotensin II type 2 receptor mediates programmed cell death. Proc Natl Acad Sci U S A 1996;93:156–60.

33. Li HW, Gao YX, Raizada MK, Sumners C. Intronic enhancement of angiotensin II type 2 receptor transgene expression *in vitro* and *in vivo*. Biochem Biophys Res Commun 2005;336:29–35.

34. Li HW, Gao YX, Matsuura T, Martynyuk A, Raizada MK, Sumners C. Adenoviral-mediated neuron specific transduction of angiotensin II type 2 receptors. Regul Pept 2005;126:213–22.

35. Marcus JS, Karackattu SL, Fleegal MA, Sumners C. Cytokine-stimulated inducible nitric oxide synthase expression in astroglia: role of Erk mitogen-activated protein kinase and NF-κB. Glia 2003;41:152–60.

36. Sidorkiewicz M, Rebas E, Szymajda M, Lawnicka H, Pawlikowski M, Lachowicz A. Angiotensin receptors in hormone-independent prostate cancer cell line DU145: presence of two variants of angiotensin type 1 receptor. Med Sci Monit 2009;15:BR106–110.

37. Li H, Gao Y, Grobe JL, et al. Potentiation of the antihypertensive action of losartan by peripheral overexpression of the ANG II type 2 receptor. Am J Physiol Heart Circ Physiol 2007;292:H727–35.

38. Ashkenazi A, Dixit VM. Death receptors: signaling and modulation. Science 1998;281:1305–08.

39. Revankar CM, Vines CM, Cimino DF, Prossnitz ER. Arrestins block G protein-coupled receptor-mediated apoptosis. J Biol Chem 2004;279:24578–84.

40. Lu Y. Transcriptionally regulated, prostate-targeted gene therapy for prostate cancer. Adv Drug Deliv Rev 2009;61:572–88.

41. Gotoh A, Ko SC, Shirakawa T, et al. Development of prostate-specific antigen promoter-based gene therapy for androgen-independent human prostate cancer. J Urol 1998;160:220–9.

42. Jarrard DF, Kinoshita H, Shi Y, et al. Methylation of the androgen receptor promoter CpG island is associated with loss of androgen receptor expression in prostate cancer cells. Cancer Res 1998;58:5310–4.

43. Carroll AG, Voeller HJ, Sugars L, Gelmann EP. p53 oncogene mutations in three human prostate cancer cell lines. Prostate 1993;23:123–34.

44. Zerbini LF, Wang Y, Correa RG, Cho JY, Libermann TA. Blockage of NF-κB induces serine 15 phosphorylation of mutant p53 by JNK kinase in prostate cancer cells. Cell Cycle 2005;4:1247–53.

AACR American Association for Cancer Research

Molecular Cancer Therapeutics

Angiotensin type 2 receptor–mediated apoptosis of human prostate cancer cells

Hongwei Li, Yanfei Qi, Chengyao Li, et al.

Mol Cancer Ther 2009;8:3255-3265. Published OnlineFirst December 8, 2009.